

1 Ocean climate change fingerprints attenuated by salt fingering?

2

3 **Gregory C. Johnson**

4 NOAA/Pacific Marine Environmental Laboratory, Seattle, Washington, USA

5

6 **Kelly A. Kearney**

7 Princeton University, Department of Geosciences, Princeton, New Jersey, USA

8

9 **Abstract**

10 Intensified double diffusive mixing may attenuate changes in ocean temperature and
11 salinity patterns from global-warming induced increases in the Earth's hydrological
12 cycle. Data from a subtropical trans-Indian Ocean survey occupied in 1987, 1995, 2002,
13 and 2009 are used to illustrate these temperature-salinity changes and to estimate the
14 intensification of double diffusive mixing driven by them. Increasingly fresher Antarctic
15 Intermediate Water together with saltier subtropical waters will tend to increase
16 destabilizing vertical salinity stratification compared to the stabilizing temperature
17 stratification. Destabilization will increase salinity (and temperature) fluxes through
18 double-diffusive salt fingering. These fluxes may act to reduce widely recognized
19 climate change fingerprints, potentially leading to underestimates of ocean changes in
20 climate studies that do not account for double-diffusive mixing.

21 **Keywords:** climate change, salt fingers, ocean mixing

22 **Index Terms:** 4215 Climate and interannual variability; 4513 Decadal ocean variability;
23 4283 Water masses; 4524 Fine structure and microstructure

1. Introduction

Models of global warming suggest that the hydrological cycle is increasing as the atmosphere warms and is able to hold and carry more moisture, and indicate that these changes in precipitation and evaporation should be large enough to be detectable in the latter 20th century [*Held and Soden, 2006*]. Evaporation dominates over precipitation in the subtropical oceans, leading to salty surface conditions there, but precipitation exceeds evaporation in the subpolar regions, leading to fresher surface conditions there [*Béranger et al., 1999*]. An increase in the hydrological cycle should lead to even saltier subtropical and fresher subpolar surface waters.

Since water in the ocean moves primarily along levels of constant potential density, σ_θ , these warmer and saltier subtropical waters overlie colder and fresher subpolar waters throughout much of the mid-latitudes, with the vertical temperature gradient acting to stabilize the water column and the vertical salinity gradient partially destabilizing it. This portion of the water column contains the Central Water [*Schmitt, 1981*]. The potential temperature–salinity (θ – S) relationship there is not linear, having a characteristic curve that is shaped by mixing associated with a double-diffusive instability called salt fingering [*Schmitt, 1981*]. This curve tends towards constant density ratio, $R_\rho = -\alpha\partial_z T/\beta\partial_z S$, where α is the thermal expansion coefficient, β the haline contraction coefficient, T temperature, and S salinity. When $R_\rho < 2$, the larger molecular diffusivity of salinity relative to temperature results in salt fingering [*Schmitt, 1981*]. The closer R_ρ approaches to 1, the stronger the mixing, and the stronger the diffusion of salt, and to a lesser extent, temperature [*St. Laurent and Schmitt, 1999*].

Cooling and freshening of subpolar waters on isopycnals and warming and salinification of subtropical waters over the last several decades has been reported in the Atlantic [Curry *et al.*, 2003], Pacific [Wong *et al.*, 1999], and South Indian [Bindoff and McDougall, 2000] Oceans. In some locations, including the South Indian Ocean, these changes may not be monotonic in parts of the water column [Bryden *et al.*, 2003]. Nonetheless, here we explore the hypothesis that changes in these water masses below and above the Central Water tend to increase the destabilizing vertical salinity gradient within the Central Water, increasing the propensity for salt fingering, and hence salinity and temperature fluxes, and that these increased fluxes may act to moderate the changes in interior ocean water property signatures imparted at the surface.

2. Data and Methods

We analyze data along a trans-Indian Ocean section from Africa to Australia sampled nominally along 32°S (Figure 1A). This section has been occupied fully three times using Conductivity-Temperature-Depth, or CTD, instruments that provide accurate and continuous vertical profiles of T and S at 2-dbar pressure (P) intervals: in Nov. – Dec. 1987 [Toole and Warren, 1993], Mar. – Apr. 2002 [McDonough *et al.*, 2008], and Mar. – May 2009. A western portion was occupied in Jun. – Jul. 1995 [Donohue and Toole, 2003] and an eastern portion in Mar. – Apr. 1995 [Talley and Baringer, 1997].

The T and S profiles are vertically low-pass filtered with a 39-point Hanning filter. Values of θ , σ_θ and Turner angle, (Tu), a measure of water column stability related to R_ρ [Ruddick, 1983], are all calculated from the filtered T and S data on the 2-dbar P grid. R_ρ is intuitive but also highly non-linear; therefore we work with Tu and convert to R_ρ for purposes of discussion and display. For this analysis, these quantities are then all

put on a regular grids for all sections, both pressure-longitude, and potential density anomaly-longitude, using linear interpolation.

Argo data used here, downloaded in February 2009, also consist of profiles of T and S versus P . Some profiles have crude automated real-time quality control applied, and some are more refined delayed mode quality controlled data. Only data of either quality control level labeled as “good” are used. Over 445,000 profiles are analyzed globally. About 500 of those are from as early as the year 1999, growing steadily in number with time to over 100,000 in 2008.

Mixed layer conditions are estimated from surface values (values from the sample closest to 10 dbar, but always between 4 and 25 dbar) of S , θ , and σ_θ from each profile. Mixed layer P , P_{ml} , is estimated as the pressure at which the linearly interpolated σ_θ of the profile is 0.03 kg m^{-3} greater than the surface value, discarding values interpolated over too large an interval. These quantities are mapped on a $1^\circ \times 1^\circ$ grid at monthly intervals using a 3-dimensional loess filter with a 500-km meridonal scale, a 1000-km zonal scale, and a 2-month time scale (disregarding year), discarding extreme outliers.

Similarly, θ , S , and P are interpolated to a fixed set of σ_θ levels for each profile, again discarding data interpolated over too large pressure intervals and extreme outliers. Retained data for each of the three parameters are mapped at each density level to a $1^\circ \times 1^\circ$ grid using a 2-D loess spatial filter (same length scales as above).

3. Results

The South Indian Ocean Central Water has very homogenous θ and S distributions on σ_θ horizons as typified by S on $\sigma_\theta = 26.75 \text{ kg m}^{-3}$, which forms a homogenous pool between about 35°S and 15°S (Figure 1A), bracketed by fresh

influences of the Indonesian Throughflow to the north and the sub-Antarctic regions to the south. Fresher Antarctic Intermediate Water (AAIW, $\sigma_\theta \sim 27.2 \text{ kg m}^{-3}$) spreads northward, overlain by the much saltier subtropical waters ($\sigma_\theta < 26 \text{ kg m}^{-3}$) with the strong destabilizing vertical salinity gradient characteristic of the Central Water in between these two contrasting water masses (Figure 1B). The South Indian Ocean Sub-Antarctic Mode Water [Wong, 2005] sits within the Central Water, as evinced by the very thick layer of relatively uniform density around $\sigma_\theta = 26.75 \text{ kg m}^{-3}$ that spreads northwestward from its origin along the winter outcrop of that isopycnal (Figure 1C).

The repeat trans-Indian Ocean sections along 32°S analyzed here afford excellent sampling of the southern portions of the South Indian Ocean Central Water. R_ρ in the upper Indian Ocean along 32°S (Figure 2A) has a local vertical minimum within the Central Water, weaker and deeper in the west ($R_\rho \sim 2.3$ near 600 dbar in 1987) and stronger and shallower in the east ($R_\rho \sim 1.5$ around 300 dbar in 1987). These low values in the east indicate conditions conducive to vigorous salt fingering [Schmitt, 1981] and, consequently, high vertical diffusivity [St. Laurent and Schmitt, 1999]. The Central Water is roughly bounded by $26.3 < \sigma_\theta < 27.1 \text{ kg m}^{-3}$, where R_ρ is relatively low (Figure 2A).

The differences of a longitude-pressure section of R_ρ in 1987 and any of those from any of the subsequent full or partial sections, for example 2009 – 1987 (Figure 2B) suggests that the R_ρ minimum has either intensified or deepened, and sometimes both, since 1987. Below its minimum and sometimes within it in the west, R_ρ generally decreases, with declines of around 0.2 or more typical near 800 dbar in the west and 700 dbar in the east. Above the minimum, and sometimes within it in the east, some

increases of a similar magnitude are evident in the 2009 R_p field (and those from other years) when compared with the 1987 values.

The longitudinal variation in R_p , as well as the availability of 1995 data only at the eastern and western ends of the 32°S section, prompt analyzing the section in three sectors: western (Africa–50°E), central (50°E–80°E), and eastern (80°E–Australia). Furthermore, since water in the ocean moves primarily along σ_θ , quantities discussed are averaged on σ_θ rather than P surfaces within each of these sectors of the section.

All three sectors display classic Central Water characteristics, with warm salty water overlying colder fresher water (Figure 3A–C). For $\sigma_\theta \sim 26.7 \text{ kg m}^{-3}$ the θ – S curves come closest to paralleling isopycnals, indicating that the vertical salinity gradient there is most strongly destabilizing relative to the vertical temperature gradient, resulting in a R_p minimum. The shapes of the curves change subtly near the cold fresh AAIW end, with the denser portions of the θ – S curves becoming colder and fresher on isopycnals with time in all of the sectors.

The 2002 section also appears to be warmer and saltier on isopycnals in the upper portion of the water column relative to the other sections, except in the eastern sector, where the upper ocean data in 1987 are warmest and saltiest. However, in the eastern sector the section latitudes differ by as much as a few degrees among the individual years. The 1987 section follows the most northerly route, closest to warm, salty subtropical influences, so some of the differences in the eastern sector may be spatial, and not temporal.

R_p is a sensitive indicator of changes in the θ – S relations, being constructed from vertical derivatives, (Figure 3D–F). The R_p minimum is least extreme in the western

sector, with values just below 2.0, suggesting only marginal propensity towards salt fingering and consequent elevated mixing [Schmitt, 1981; St. Laurent and Schmitt, 1999]. However, the R_ρ minimum in the western sector moves towards generally denser horizons and strengthens slightly from 1987 at least through 2002, suggesting the possibility of more mixing with time there, albeit with a partial return to a weaker minimum in 2009. In the central sector, the R_ρ minimum is stronger than in the west, near 1.6, suggesting stronger salt fingering activity. It moves to denser horizons from 1987 to 2002 in the central sector, staying roughly fixed between 2002 and 2009. In the eastern sector, the R_ρ minimum is strongest, approaching 1.5 on average, with no consistent pattern of change in either strength or isopycnal level among the 4 occupations of the section. This very low R_ρ minimum suggests quite strong salt fingering and elevated mixing in the eastern sector Central Water.

4. Discussion

One possible interpretation of these patterns is that in the east where salt fingering is strong in all years, changes in the θ - S properties of the Central Water may be rapidly moderated by strong vertical mixing, keeping the θ - S curves (and hence the associated values of R_ρ) relatively invariant in time. In the central region, where salt fingering activity is weaker but still present, the cooling and freshening of the AAIW with time has moved the R_ρ minimum to denser horizons, but not strengthened it, so moderate mixing is working its way down toward the freshening and cooling AAIW. In the western region, where the R_ρ minimum is weakest, the changing AAIW has not only moved the R_ρ minimum to denser horizons, but also shifted that portion of the water column towards

lower R_p values and more salt fingering activity since 1987, potentially moving towards moderation of the upper reaches of the AAIW changes.

The effects of these R_p patterns and changes on mixing can be estimated by applying a diffusivity parameterization following *Johnson* [2006] to the data from each section to estimate vertical salt and temperature fluxes, and from those fluxes find tendencies, on density surfaces (Figure 4). These tendency estimates are noisy, but sector average patterns are still clear. In the western sector, the R_p minima are too high in 1987 to effect any mixing over background levels; there is a slight tendency for salinification (and heating) for densities greater than the R_p minimum post-1987 and a slight tendency for freshening (and cooling) for densities less than the R_p minimum post-1987. In the central sector the tendency towards salinification and warming for densities greater than the R_p minimum and towards freshening and cooling at lighter densities is stronger. In the eastern sector the pattern is even stronger. These tendencies are highest on the edges of the Sub-Antarctic Mode Water, where property curvatures are elevated. Higher tendencies for $\sigma_\theta < 26.5 \text{ kg m}^{-3}$ in the eastern and central sections are associated with the seasonal thermocline, and will not be discussed further here.

In the eastern sector the S and θ tendencies estimated within the Central Water can exceed $\pm 0.02 \text{ PSS-78 yr}^{-1}$ and $0.1^\circ\text{C yr}^{-1}$. They roughly cancel in their contributions to vertical density flux. These tendencies are on the order of rates of previously reported decadal changes in S and θ on isopycnals in the region [*Bindoff and McDougall*, 2000; *Bryden et al.*, 2003]. This result opens the possibility that salt-fingering driven vertical mixing could moderate such climate signals, especially if freshening of subpolar waters and salinification of subtropical waters over time act to decrease R_p further.

Interior changes in ocean properties such as θ and S can be useful in diagnosing climate changes at the ocean surface [Bindoff and McDougall, 1994] and are robust fingerprints of such global climate change in models [Banks *et al.*, 2000]. Ocean changes of salinity within isopycnal layers of the past few decades have been used to estimate the size of decadal increases in the hydrological cycle over the ocean [Helm *et al.*, 2009]. If these increases in the hydrological cycle increase the destabilizing salinity gradient and hence vertical mixing, as illustrated here, elevated vertical salt and temperature fluxes, as estimated here, may be of sufficient magnitude to moderate this climate signature imparted at the ocean surface as it travels into the interior by transferring increasing amounts of heat and salt downward across isopycnals, making layers that were cooled and freshened at the surface warmer and saltier in the interior, and vice versa. Hence, accounting for diapycnal processes like increased mixing owing to salt fingering in climate change studies could improve their diagnostic skill.

Acknowledgments

GCI and KAK worked on this analysis during the U.S. CO₂/Repeat Hydrography Program 2009 occupation of the 32°S trans-Indian Ocean section. The NOAA Office of Oceanic and Atmospheric Research and the NOAA Climate Program Office funded GCI. The National Science Foundation Division of Ocean Sciences funded KAK under Grant NSF OCE-0223869. Float data used here were collected and made freely available by Argo (a pilot program of the Global Ocean Observing System) and contributing national programs (<http://www.argo.net/>). We thank all those who helped to collect data for each 32°S trans-Indian Ocean section. PMEL Contribution #3333.

References

- Banks, H., R. Wood, J. Gregory, T. Johns, and G. Jones (2000), Are observed decadal changes in intermediate water masses a signature of anthropogenic climate change?, *Geophys. Res. Lett.*, *27*, 2961–2964.
- Beránger, K., L. Siefridt, B. Barnier, E. Garnier, and H. Roquet (1999), Evaluation of operational ECMWF surface freshwater fluxes of oceans during 1991–1997, *J. Mar. Systems*, *22*, 13–36.
- Bindoff, N. J., and T. J. McDougall (1994), Diagnosing climate-change and ocean ventilation using hydrographic data, *J. Phys. Oceanogr.*, *24*, 1137–1152.
- Bindoff, N. J., and T. J. McDougall (2000), Decadal changes in an Indian Ocean Section at 32°S and their interpretation, *J. Phys. Oceanogr.*, *30*, 1207–1222.
- Bryden, H. L., E. L. McDonough, and B. A. King (2003), Changes in ocean water mass properties: Oscillations or trends?, *Science*, *300*, 2086–2088.
- Curry, R., B. Dickson, and I. Yashayaev (2003), A change in the freshwater balance of the Atlantic Ocean over the past four decades, *Nature*, *426*, 826–829.
- Donohue, K. A., and J. M. Toole (2003), A near-synoptic survey of the Southwest Indian Ocean, *Deep-Sea Res. II*, *50*, 1893–1931.
- Held, I. M., and B. J. Soden (2006), Robust response of the hydrological cycle to global warming, *J. Climate*, *19*, 5686–5699.
- Helm, K. P., N. L. Bindoff, and J. A. Church (2009), Global hydrological-cycle changes inferred from observed ocean salinity, *Nature Geosci.*, submitted.
- Johnson, G. C. (2006), Generation and initial evolution of a mode water θ -S anomaly, *J. Phys. Oceanogr.*, *36*, 739–751.

228 McDonough, E. L., H. L. Bryden, B. A. King, and R. A. Saunders (2008), The circulation
 229 of the Indian Ocean at 32°S, *Prog. Oceanogr.*, 29, 20–36.
 230 Ruddick, B. (1983), A practical indicator of the stability of the water column to double-
 231 diffusive activity, *Deep-Sea Res.*, 10A, 1105–1107.
 232 Schmitt, R. W. (1981), Form of the temperature-salinity relationship in the central water:
 233 Evidence for double-diffusive mixing, *J. Phys. Oceanogr.*, 11, 1015–1026.
 234 St. Laurent, L., and R. W. Schmitt (1999), The contribution of salt fingers to vertical
 235 mixing in the North Atlantic Tracer Release Experiment, *J. Phys. Oceanogr.*, 29,
 236 1404–1424.
 237 Talley, L. D., and M. O. Baringer (1997), Preliminary results from WOCE hydrographic
 238 sections at 80°E and 32°S in the central Indian Ocean, *Geophys. Res. Lett.*, 24,
 239 2789–2792.
 240 Toole, J. M., and B. A. Warren (1993), A hydrographic section across the subtropical
 241 South Indian Ocean, *Deep-Sea Res. I*, 40, 1973–2019.
 242 Wong, A. P. S. (2005), Subantarctic Mode Water and Antarctic Intermediate Water in the
 243 South Indian Ocean based on profiling float data 2000–2004, *J. Mar. Res.*, 63,
 244 789–812.
 245 Wong, A. P. S., N. L. Bindoff, and J. A. Church (1999), Large-scale freshening of
 246 intermediate waters in the Pacific and Indian Oceans, *Nature*, 400, 440–443.
 247

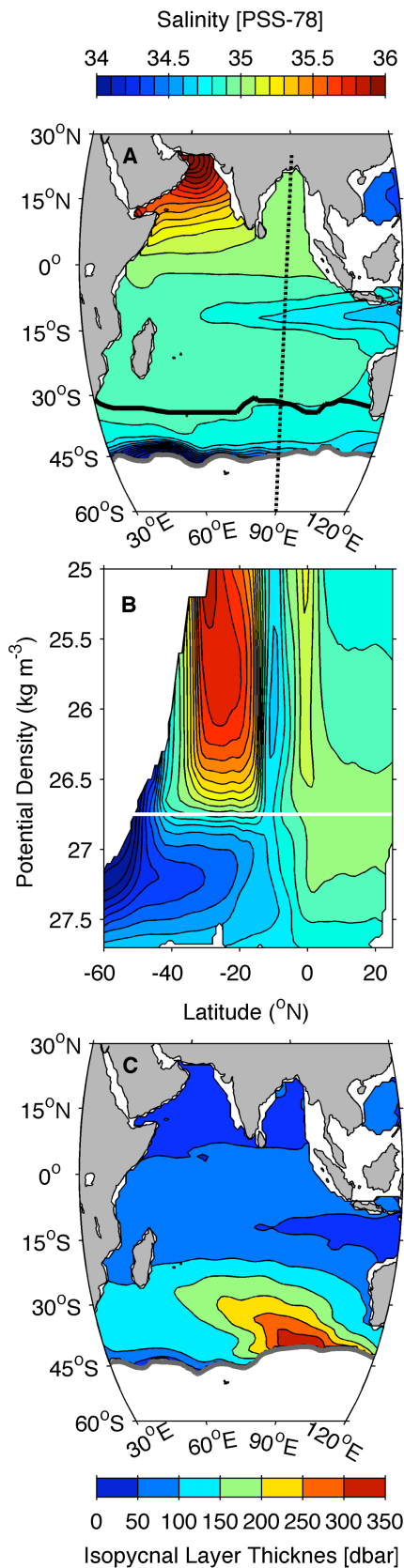


Figure 1. (A) Salinity (S) map on potential isopycnal $\sigma_0 = 26.75 \text{ kg m}^{-3}$ from Argo data color contoured at 0.1 PSS-78 intervals (top color bar) with locations of 2009 trans-Indian Ocean section (black line), Figure 1B meridional transect (dashed line), and this isopycnal in winter (grey line). (B) Latitude- σ_0 section of S contoured at 0.1 PSS-78 intervals (top color bar) along 90°E with values lighter than wintertime surface densities masked and $\sigma_0 = 26.75 \text{ kg m}^{-3}$ (white line) used in Figure 1A indicated. (C) Map of thickness of the layer $26.7 < \sigma_0 < 26.8 \text{ kg m}^{-3}$ from Argo data color contoured at 50 dbar intervals (bottom color bar).

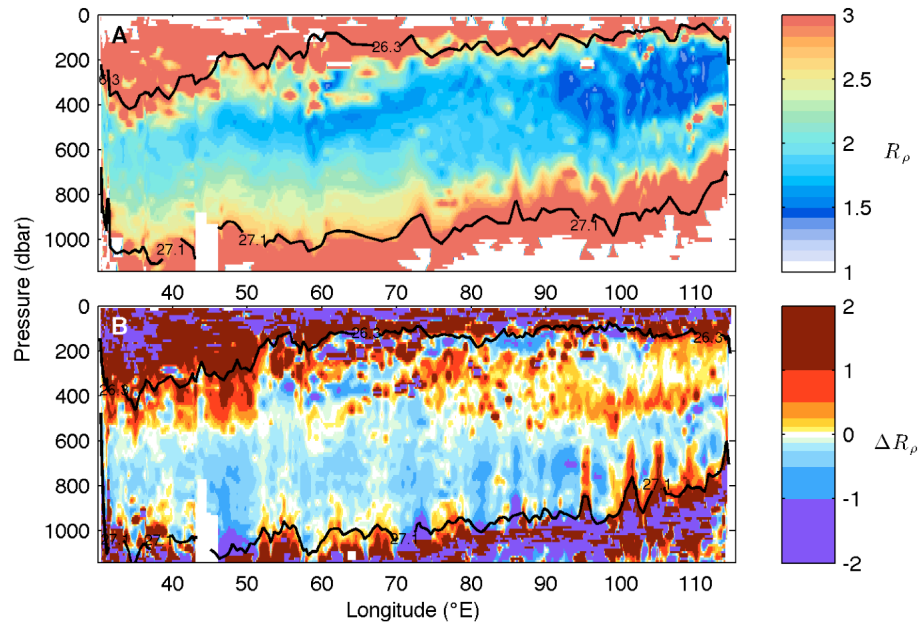


Figure 2. (A) Longitude-pressure section of density ratio (R_ρ) estimated from data from the 1987 occupation of a trans-Indian Ocean section along nominal latitude 32°S (see Figure 1A for location). Potential isopycnals $\sigma_\theta = 26.3$ and 27.1 kg m^{-3} approximately bounding the Central Water are indicated by black contours. (B) Section of 2009 – 1987 difference of density ratio (ΔR_ρ) with these same isopycnals, but for 2009, indicated by black contours.

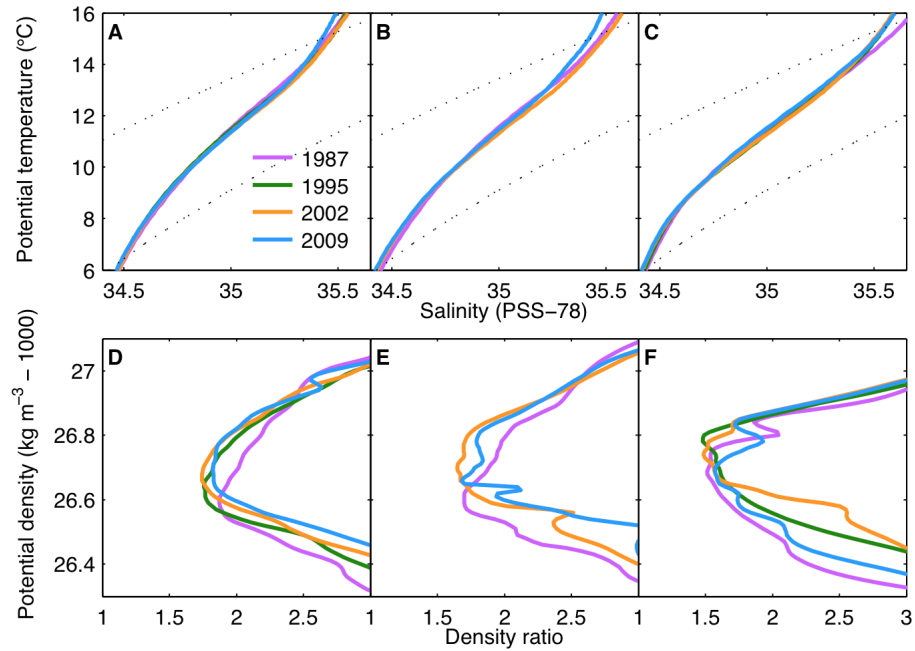
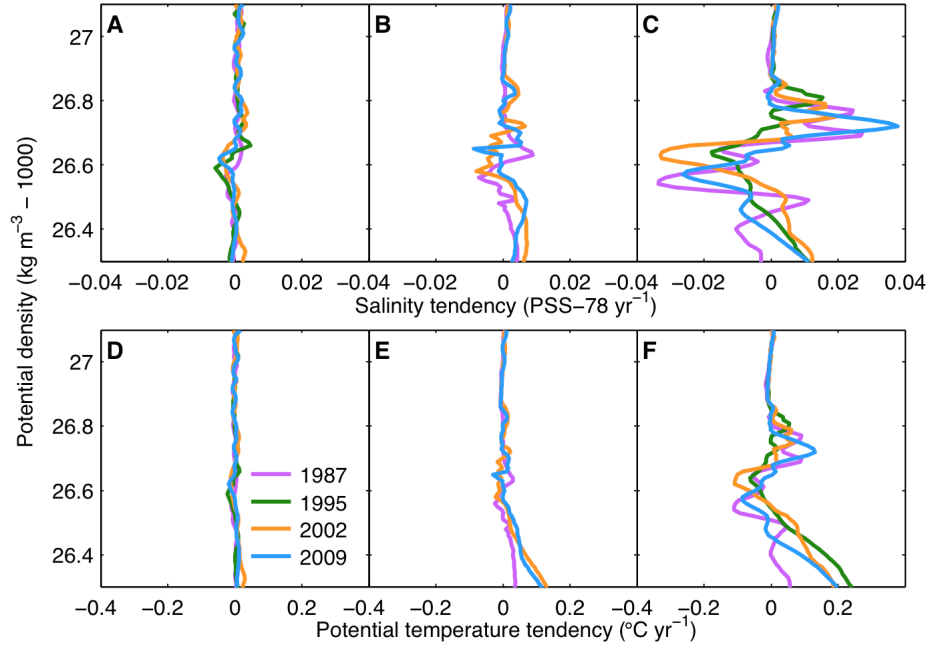


Figure 3. (A, B, C): Potential temperature – salinity (θ – S) curves averaged on potential density (σ_θ) surfaces over three longitude ranges with $\sigma_\theta = 26.3$ and 27.1 kg m^{-3} indicated by dashed lines. Data from the three complete and one partial modern occupations of the trans-Indian Ocean section nominally along 32°S are used. Line colors differentiate years (legend). (D, E, F): Analogous averages of R_ρ on σ_θ surfaces. Longitude ranges span western (Africa– 50°E ; A, D), central (50°E – 80°E ; B, E), and eastern (80°E –Australia; C, F) sectors of the section.



292

293 **Figure 4.** (A, B, C): Average vertical salinity tendencies (PSS-78 yr⁻¹) on σ_θ horizons
 294 estimated by applying a diffusivity parameterization to data from the three complete and
 295 one partial modern occupations of a trans-Indian Ocean section nominally along 32°S.
 296 Line colors differentiate years (legend). (D, E, F): Analogous averages of vertical
 297 potential temperature tendencies (°C yr⁻¹). Longitude ranges span the western (Africa–
 298 50°E; A, D), central (50°E–80°E; B, E), and eastern (80°E–Australia; C, F) sectors of the
 299 section.